Infrared Spectrum of the Hyponitrite Dianion, $N_2O_2^{2-}$, Isolated and Insulated from Stabilizing Metal Cations in Solid Argon

Lester Andrews* and Binyong Liang

Contribution from the University of Virginia, Department of Chemistry, Charlottesville, Virginia 22904-4319

Received August 7, 2000

Abstract: Ultraviolet irradiation of a rigid 7 K argon matrix containing alkali or alkaline earth metal atoms and $(NO)_2$ isolated from each other by one or two layers of argon forms $N_2O_2^{2-}$ dianions insulated from two M^+ cations by argon atoms, and visible photolysis reverses this electron-transfer process likely involving the $N_2O_2^-$ anion intermediate. The isolated $N_2O_2^{2-}$ dianion is identified from isotopic substitution and isotopic mixtures, which show that the new 1028.5 cm^{-1} metal independent absorption involves two equivalent NO subunits. DFT calculations predict a strong 1078.1 cm^{-1} fundamental for the $Li(NO)_2Li$ molecule and isotopic frequency ratios in excellent agreement with the observed values, which provides a model for the matrix dianion system. The spectrum of solid $Na_2N_2O_2$ exhibits a 1030 cm^{-1} infrared band, which strongly supports the present $N_2O_2^{2-}$ dianion assignment. The electrostatic stabilization of $N_2O_2^{2-}$, which is probably unstable in the gas phase, is made possible by metal cations separated by one or two insulating layers of argon in the rigid 7 K matrix.

Introduction

Dianions are ubiquitous in crystalline solids, and common examples in mineralogy include oxide (O^{2-}), carbonate (CO_3^{2-}), and sulfate (SO_4^{2-}).[1] In the solid phase the counterions necessary to stabilize dianions are in adjacent sites in the crystal lattice. However, there is no firm evidence for atomic and diatomic dianions in the gas phase, but larger molecular dianions have been observed.[2,3] Although atoms and most small molecules have an affinity for electrons and capture one electron in an exothermic process, a second electron is repulsive and the acquisition of a second electron is an endothermic process.[2,4] Even CO_3^{2-} and SO_4^{2-} are not large enough to be stable in the gas phase because of the strong Coulomb repulsion between the two excess electrons.[2,5,6] However, larger dianions are often stable and examples recently observed by photodetachment photoelectron spectroscopy in the gas phase include dicarboxylate, PtX_4^{2-}, and the heavy transition metal MX_6^{2-} dianions (X = Cl, Br).[3,7−10] Nevertheless, stable dianions are often short-lived: the recently observed MF_4^{2-} (M = Be, Mg) dianions have lifetimes in the 0.1 ms range.[11] How then can we prolong the lifetime and investigate the properties of a small dianion isolated from perturbations of the adjacent cations that are required to stabilize it?

The matrix isolation technique has been employed to study molecular anions both as isolated anions surrounded by at least one layer of matrix atoms and as ion pairs where cation and anion are electrostatically bound together. The latter includes $M^+O_2^-$ alkali superoxide, $M^+O_3^-$ alkali ozonide, and $M^+NO_2^-$ ion-pair molecules[12−14] prepared in atom-molecule reactions, and the former includes isolated O_3^- and NO_2^- made by the capture of electrons from a photoionization process.[15,16] Anion spectra in the $M^+O_2^-$, $M^+O_3^-$, and $M^+NO_2^-$ molecules show a clear dependence on the geminate metal cation; however, the isolated anion spectra are independent of the electron source. In fact both $M^+NO_2^-$ and isolated NO_2^- have been formed in the same sample.[14] Several small dianions, including O_2^{2-}, NO^{2-}, carbonate, and sulfite, have been investigated by matrix isolation spectroscopy.[12,17−19] The $Li^+(O_2^{2-})Li^+$ and $Li^+(NO^{2-})Li^+$ ion-trio species have been identified in the matrix systems from isotopic shifts.[12,17] Subsequent DFT calculations in this laboratory have confirmed these bonding descriptions.[20] A carbonate moiety has been prepared by the reaction of thallium suboxide (Tl_2O) and carbon dioxide (CO_2) in the condensing matrix gas as the molecule $(Tl^+)(CO_3^{2-})(Tl^+)$, which is trapped in the solid matrix. The carbonate dianion spectrum reveals perturbations by the adjacent thallous cations.[18]

(1) Cotton, F. A.; Wilkinson, G.; Murillo, C. A.; Bochmann, M. *Advanced Inorganic Chemistry*, 6th ed.; Wiley: New York, 1999.
(2) Scheller, M. K.; Compton, R. N.; Cederbaum, L. S. *Science* **1995**, *270*, 1160.
(3) Wang, L. S.; Wang, X. B. *J. Phys. Chem. A* **2000**, *104*, 1978 and references therein.
(4) Hotop, H.; Lineberger, W. C. *J. Phys. Chem. Ref. Data* **1985**, *14*, 731.
(5) Boldyrev, A. I.; Simons, J. *J. Phys. Chem.* **1994**, *98*, 2298.
(6) Boldyrev, A. I.; Gutowski, M.; Simons, J. *Acc. Chem. Res.* **1996**, *29*, 497.
(7) Wang, X. B.; Wang, L. S. *J. Chem. Phys.* **1999**, *111*, 4497.
(8) Ding, C. F.; Wang, X. B.; Wang, L. S. *J. Phys. Chem. A* **1998**, *102*, 8633.
(9) Wang, X. B.; Wang, L. S. *J. Am. Chem. Soc.* **2000**, *122*, 2339.
(10) Skurski, P.; Simons, J.; Wang, X. B.; Wang, L. S. *J. Am. Chem. Soc.* **2000**, *122*, 4499.
(11) Middleton, R.; Klein, J. *Phys. Rev. A* **1999**, *60*, 3515.
(12) Andrews, L. *J. Am. Chem. Soc.* **1968**, *90*, 7368. Andrews, L. *J. Chem. Phys.* **1969**, *50*, 4288.
(13) Spiker, R. C., Jr.; Andrews, L. *J. Chem. Phys.* **1973**, *59*, 1851.
(14) Milligan, D. E.; Jacox, M. E. *J. Chem. Phys.* **1971**, *55*, 3404.
(15) Milligan, D. E.; Jacox, M. E.; Guillory, W. A. *J. Chem. Phys.* **1970**, *52*, 3864.
(16) Andrews, L.; Ault, B. S.; Grzybowski, J. M.; Allen, R. O. *J. Chem. Phys.* **1975**, *62*, 2461.
(17) Tevault, D. E.; Andrews, L. *J. Phys. Chem.* **1973**, *77*, 1640 (Li + NO).
(18) David, S. J.; Ault, B. S. *J. Phys. Chem.* **1982**, *86*, 4618.
(19) David, S. J.; Ault, B. S. *Inorg. Chem.* **1984**, *23*, 1211.
(20) Andrews, L.; Zhou, M. F.; Wang, X. *J. Phys. Chem. A* **2000**, *104*, 8475 (Tl + NO).

10.1021/ja0029331 CCC: $20.00
Published on Web 02/10/2001

Alkali and other metal hyponitrites are known in the solid phase, and evidence has been presented for both *cis*- and *trans*-hyponitrite anion structures; however, these compounds are unstable.[21−24] A hyponitrite species is suggested to form on solid MgO based on infrared spectra following the adsorption of NO.[25] In laser-ablation experiments with Mg, Ca, and NO, a sharp, weak 1028.5 cm^{-1} absorption appeared on ultraviolet photolysis.[26] The isotopic shifts and splittings for this absorption and its agreement with the spectrum of sodium hyponitrite[21−23] suggested a hyponitrite species.

To prepare a small isolated dianion, a rigid matrix host cage and the electrostatic stabilization of counterions separated by one or two matrix gas layers from the dianion guest are needed. This requires the isolation of separate metal atoms and electron receptor guests followed by appropriate radiation to transfer valence electrons. Here we describe such experiments to prepare the isolated hyponitrite dianion $N_2O_2^{2-}$ for the first time.

Experimental and Theoretical Methods

The laser-ablation matrix isolation apparatus and experiment have been described in previous reports.[27−29] Metal targets (Li, Na, Mg, Ca, Ba) positioned 2 cm from the cold window were ablated by focused 1064 nm radiation from a pulsed YAG laser. Nitric oxide (Matheson) samples were prepared after fractional distillation from a coldfinger; ^{15}NO (MSD Isotopes, 99% ^{15}N) was treated similarly; $^{15}N^{18}O$ (Isotec, 99.9% ^{15}N, 98.5% ^{18}O) was used as received. A Nicolet 550 FTIR instrument operating at 0.5 cm^{-1} resolution (frequency accuracy ±0.1 cm^{-1}) with a liquid nitrogen cooled HgCdTe detector was used to record spectra. The instrument was purged continuously with a Balston 75−20 compressed air-dryer. Matrix samples were co-deposited on a 7 K CsI window, irradiated by filtered light from a medium-pressure mercury lamp (Philips, 175 W) with the globe removed or a tungsten lamp (Wiko, 90 W), and more spectra were collected.

Density functional theory (DFT) calculations were performed on potential product molecules by using the Gaussian 94 program system.[30] Most calculations employed the hybrid B3LYP functional but comparisons were done with the BPW91 functional as well.[31,32] The 6-311+G* basis set was used for N, O, and metal atoms.[33,34] Geometries were fully optimized and the vibrational frequencies computed by using analytical second derivatives.

Results and Discussion

The new absorptions observed here will be identified by isotopic substitution and comparison with DFT calculated isotopic frequencies.

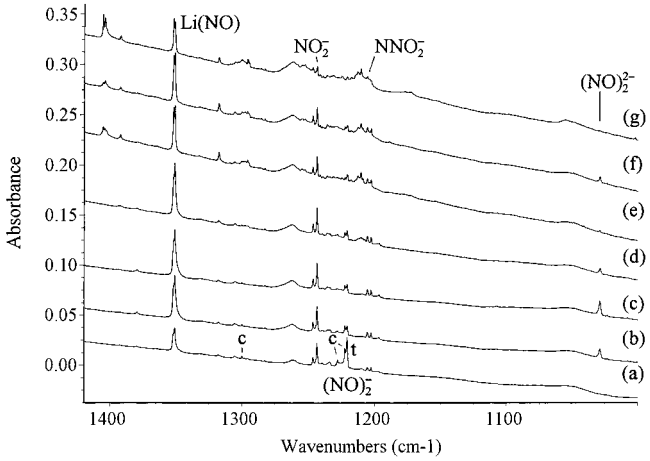

Figure 1. Infrared spectra in the 1420−1000 cm^{-1} region for laser-ablated lithium co-deposited with 0.4% NO in argon at 7 K: (a) spectrum of sample deposited for 70 min, 256 scans, (b) spectrum after $\lambda > 240$ nm photolysis for 15 min, 192 scans, (c) spectrum after 240−380 nm photolysis for 15 min, 128 scans, (d) spectrum after annealing to 25 K, 128 scans, (e) spectrum after annealing to 35 K, 128 scans, (f) spectrum after 240−380 nm photolysis, 256 scans, and (g) spectrum after 40 K annealing, 256 scans.

Alkali Metals. Figure 1 shows the 1420−1000 cm^{-1} region of the spectrum from a sample prepared by co-depositing laser-ablated lithium and 0.4% NO in argon at 7 K. The strong 1351.0 cm^{-1} band has been assigned to Li(NO) in three previous investigations by using thermal lithium atoms.[14,17,35] The sharp 1589.3, 1243.7, and 1221.0 cm^{-1} and weak 1300.3, 1221.7, and 1205.0 cm^{-1} absorptions observed in a large number of laser-ablation experiments with NO are due to isolated $(NO)_2^+$, NO_2^-, *trans*-$(NO)_2^-$, *cis*-$(NO)_2^-$, and NNO_2^-, respectively.[14,36] The relative absorbance of *trans*-$(NO)_2^-$ is 4−6 times greater than that for $(NO)_2^+$ with Li and Na whereas with transition metals the $(NO)_2^+$ absorption is substantially stronger (10 times for Ni).[36,37] Not shown are strong 795.3 and 650.7 cm^{-1} bands due to $Li^+(NO^{2-})Li^+$ and Li(NO), respectively,[17] and a weak NO_2 band at 1610.8 cm^{-1}. Irradiation with the full light of a medium-pressure mercury arc lamp ($\lambda > 240$ nm) produced a sharp weak 1028.5 cm^{-1} absorption (Figure 1b) and decreased the 1221.0 cm^{-1} absorption of *trans*-$(NO)_2^-$. It was noticed that the 1028.5 cm^{-1} peak intensity decreased during the recording of the scans, which suggested that visible light from the infrared source might destroy the species responsible for the new 1028.5 cm^{-1} absorption. Further irradiation employed a 240−380 nm transmitting black filter and the 1028.5 cm^{-1} absorption was stronger (Figure 1c). Annealing to 25 K markedly decreased the 1028.5 cm^{-1} absorption and increased the 1351.0 cm^{-1} band, and annealing to 35 K virtually destroyed the 1028.5 cm^{-1} band and produced new 1404.1 and 1392.6 cm^{-1} features. Another 240−380 nm irradiation (Figure 1f) brought back some of the 1028.5 cm^{-1} absorption, but final annealing to 40 K destroyed it (Figure 1g).

Figure 2 illustrates the 1410−1000 cm^{-1} region of the spectrum of a matrix containing laser-ablated sodium and 0.4% NO. The strong 1358.3 cm^{-1} band is due to Na(NO).[14,38] The same NO_2^- and $(NO)_2^-$ bands are observed.[14,36] Full-arc

(21) Kuhn, L.; Lippincott, E. R. *J. Am. Chem. Soc.* **1956**, *78*, 1820.
(22) Miller, D. J.; Polydropoulos, C. N.; Watson, D. *J. Chem. Soc.* **1960**, 687.
(23) McGraw, G. E.; Bernitt, D. L.; Hisatsune, I. C. *Spectrochim. Acta* **1967**, *23A*, 25.
(24) Laane, J.; Ohlsen, J. R. *Prog. Inorg. Chem.* **1980**, *27*, 465.
(25) Cerruti, L.; Modone, E.; Guglielminotti, E.; Borello, E. *J. Chem. Soc., Faraday Trans. 1* **1974**, *70*, 729.
(26) Kushto, G. P.; Ding, F.; Liang, B.; Wang, X.; Citra, A.; Andrews, L. *Chem. Phys.* **2000**, *257*, 223.
(27) Burkholder, T. R.; Andrews, L. *J. Chem. Phys.* **1991**, *95*, 8697.
(28) Hassanzadeh, P.; Andrews, L. *J. Phys. Chem.* **1992**, *96*, 9177.
(29) Zhou, M. F.; Andrews, L. *J. Am. Chem. Soc.* **1998**. *120*, 13230.
(30) *Gaussian 94, Revision B.1*; Frisch, M. J.; Trucks, G. W.; Schlegel, H. B.; Gill, P. M. W.; Johnson, B. G.; Robb, M. A.; Cheeseman, J. R.; Keith, T.; Petersson, G. A.; Montgomery, J. A.; Raghavachari, K.; Al-Laham, M. A.; Zakrzewski, V. G.; Ortiz, J. V.; Foresman, J. B.; Cioslowski, J.; Stefanov, B. B.; Nanayakkara, A.; Challacombe, M.; Peng, C. Y.; Ayala, P. Y.; Chen, W.; Wong, M. W.; Andres, J. L.; Replogle, E. S.; Gomperts, R.; Martin, R. L.; Fox, D. J.; Binkley, J. S.; Defrees, D. J.; Baker, J.; Stewart, J. P.; Head-Gordon, M.; Gonzalez, C.; Pople J. A., Gaussian, Inc.: Pittsburgh, PA, 1995.
(31) Lee, C.; Yang, E.; Parr, R. G. *Phys. Rev. B* **1988**, *37*, 785.
(32) Perdew, J. P. *Phys. Rev. B* **1986**, *33*, 8822. Becke, A. D. *J. Chem. Phys.* **1993**, *98*, 5648.
(33) McLean, A. D.; Chandler, G. S. *J. Chem. Phys.* **1980**, *72*, 5639.
(34) Krishnan, R.; Binkley, J. S.; Seeger, R.; Pople, J. A. *J. Chem. Phys.* **1980**, *72*, 650.
(35) Andrews, W. L. S.; Pimentel, G. C. *J. Chem. Phys.* **1966**, *44*, 2361.
(36) Andrews, L.; Zhou, M. F.; Willson, S. P.; Kushto, G. P.; Snis, A.; Panas, I. *J. Chem. Phys.* **1998**, *109*, 177.
(37) Zhou, M. F.; Andrews, L. *J. Phys. Chem. A* **2000**, *104*, 3915 (Fe, Co, Ni + NO).
(38) Tevault, D. E.; Andrews, L. *J. Phys. Chem.* **1973**, *77*, 1646 (Na + NO).

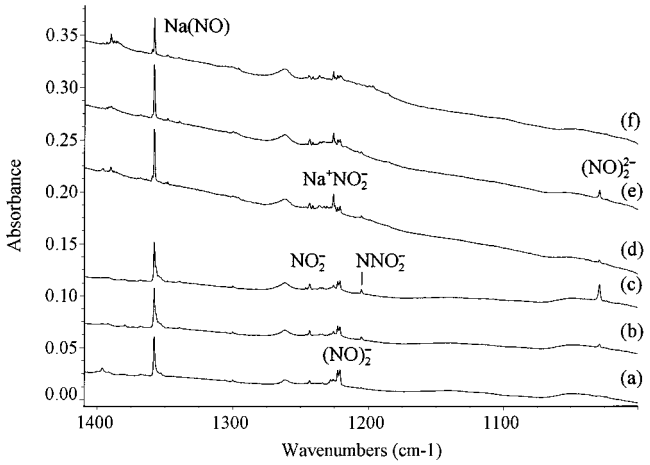

Figure 2. Infrared spectra in the 1410−1000 cm^{-1} region for laser-ablated sodium co-deposited with 0.4% NO in argon at 7 K: (a) spectrum of sample deposited for 70 min, 256 scans, (b) spectrum after $\lambda > 240$ nm photolysis for 15 min, 64 scans, (c) spectrum after 240−380 nm photolysis for 15 min, 64 scans, (d) spectrum after annealing to 35 K, 64 scans, (e) spectrum after 240−380 nm photolysis, 64 scans, and (f) spectrum after 40 K annealing, 256 scans.

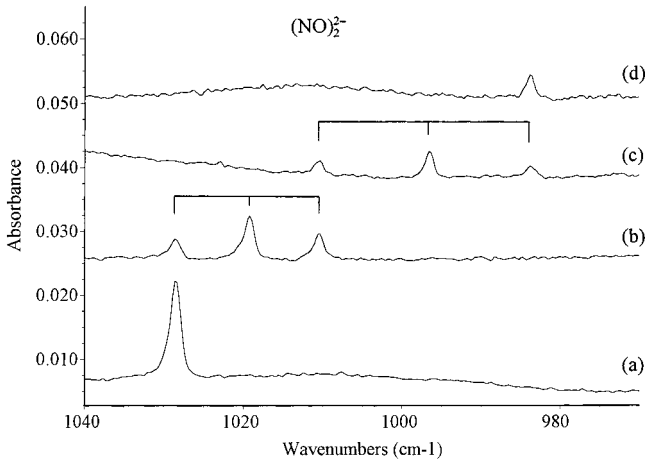

Figure 3. Infrared spectra in the 1040−960 cm^{-1} region for laser-ablated metals co-deposited with isotopic nitric oxide in argon at 7 K after ultraviolet photolysis for 15 min: (a) Na + 0.4% $^{14}N^{16}O$, (b) Na + 0.2% $^{14}N^{16}O$ + 0.2% $^{15}N^{16}O$, (c) Mg + 0.2% $^{15}N^{16}O$ + 0.2% $^{15}N^{18}O$, and (d) Mg + 0.3% $^{15}N^{18}O$.

irradiation produced a weak 1028.5 cm^{-1} band and reduced the *trans*-$(NO)_2^-$ absorption, but 240−380 nm irradiation gave a much stronger 1028.5 cm^{-1} absorption (Figure 2b,c) and reduced the 1776.2 cm^{-1} $(NO)_2$ band absorbance by 2%. Annealing to 35 K almost destroyed the 1028.5 cm^{-1} band and produced a new 1390.6 cm^{-1} absorption (Figure 2d) and increased a weak band at 1225.8 cm^{-1} probably due[14] to $Na^+NO_2^-$. Another 240−380 nm photolysis again reproduced most of the 1028.5 cm^{-1} band, but final 40 K annealing destroyed it (Figure 2 e,f). The sodium spectra with $^{14}N^{16}O$ and $^{14}N^{16}O$ + $^{15}N^{16}O$ are shown in Figure 3 a,b; the sharp triplet mixed isotopic absorption at 1028.5, 1019.2, and 1010.4 cm^{-1} clearly demonstrates the involvement of two equivalent nitrogen atoms in this vibrational mode.

Alkaline Earth Metals. Experiments were done with Mg, Ca, and Ba and isotopic modifications of NO. The 1028.5 cm^{-1} band was observed after ultraviolet photolysis ($\lambda > 240$ nm) in all of these experiments and it disappeared on annealing to 35 K; the band was regenerated in part on subsequent UV photolysis. The mixed $^{15}N^{16}O$ + $^{15}N^{18}O$ experiment with Mg is shown in Figure 3c; the 1010.4, 996.5, and 983.7 cm^{-1} triplet indicates the involvement of two equivalent oxygen atoms. Finally, the pure $^{15}N^{18}O$ isotopic sample gave a single band at 983.7 cm^{-1}.

Table 1. Infrared Absorptions (cm^{-1}) Observed for Reactions of Laser-Ablated Li and Na with NO in Excess Argon

$^{14}N^{16}O$	$^{15}N^{16}O$	$^{15}N^{18}O$	identification
1589.3	1561.9	1520.3	$(NO)_2^+$
1404.1	1381.4	1344.1	$(Li(Ar)_x(NO)_2(Ar)_xLi)$
1392.6			$(Li(Ar)_x(NO)_2(Ar)_xLi)$ site
1390.6	1366.6		$(Na(Ar)_x(NO)_2(Ar)_xNa)$
1358.3			Na(NO)
1351.0	1327.7	1291.6	Li(NO)
1300.3	1278.9	1242.7	c-$(NO)_2^-$
1243.7	1218.3	1191.9	NO_2^-
1222.7	1198.6	1172.0	c-$(NO)_2^-$
1221.0	1199.9	1167.4	t-$(NO)_2^-$
1028.5	1010.4	983.7	$N_2O_2^{2-}$
795.3	790.0	785.0	Li(NO)Li
690.0	690.0	674.1	? broad
650.7	649.8	643.9	Li(NO)

Table 2. Photochemical Behavior of Three Important $(NO)_2^q$ Absorptions (cm^{-1}) in the Ba + NO Experiment[a]

action	1776.2[b]	1221.0[c]	1028.5[d]
deposition	30	3.5	0.0
$240 < \lambda < 380$ nm	26	5.5	4.6
$\lambda > 380$ nm	25	6.0	2.0
$240 < \lambda < 380$ nm	24	6.1	4.6
$\lambda > 290$ nm	25	7.3	3.7
$240 < \lambda < 380$ nm	24	6.6	4.0
W lamp, $\lambda > 630$ nm	25	7.3	0.0
$240 < \lambda < 380$ nm	24	6.8	3.8
anneal to 35 K	150	3.4	1.2

[a] Absorbances listed in mau (au × 1000). [b] $q = 0$. [c] $q = -1$. [d] $q = -2$.

The barium experiment explored different photolysis wavelengths. First, 240−380 nm photolysis for 20 min produced the new sharp 1028.5 cm^{-1} band (0.0046 absorbance units, au), decreased the 1776.2 cm^{-1} $(NO)_2$ band from 0.030 to 0.026 au, and increased the 1221.0 cm^{-1} $(NO)_2^-$ band from 0.0035 to 0.0055 au. The next $\lambda > 380$ nm photolysis decreased the 1028.5 cm^{-1} band to 0.0020 au and increased the 1221.0 cm^{-1} band to 0.0060 au. A subsequent 240−380 nm photolysis restored the 1028.5 cm^{-1} band and decreased the 1776.2 cm^{-1} band to 0.024 au. A low-intensity tungsten lamp ($\lambda > 630$ nm, red + near-IR) photolysis also destroyed the 1028.5 cm^{-1} band and increased the 1776.2 cm^{-1} band to 0.025 au and the 1221.0 cm^{-1} band to 0.0073 au. A final 240−380 nm irradiation again reversed the process giving 0.0038 au for the 1028.5 cm^{-1} band and 0.024 au for the 1776.2 cm^{-1} absorption. A final annealing to 35 K reduced the 1028.5 cm^{-1} band to 0.0012 au and increased the 1776.2 cm^{-1} band to 0.115 au. The band absorbances are collected in Table 2.

Group 13 Metals. A new 1028.5 cm^{-1} band (0.002 au) was produced on deposition of a Tl + NO sample; this band disappeared on annealing to 25 K and was almost regenerated on $\lambda > 240$ nm photolysis.[20] A weak 1028.5 cm^{-1} band appeared on UV photolysis in Al + NO experiments.[39]

Calculations. DFT calculations with the B3LYP functional were performed on $^3A''$ Li(NO) and Na(NO), and the results are given in Table 3. The calculated frequencies for the N−O mode, 1391.4 and 1378.6 cm^{-1}, differ by −12.8 cm^{-1} compared to the +7.3 cm^{-1} difference between the observed 1351.0 and

(39) Andrews, L.; Zhou, M. F.; Bare, W. D. *J. Phys. Chem. A* **1998**, *102*, 5019.

Table 3. Calculated Geometries and Isotopic Frequencies for M(NO), M(NO)M, $M(NO)_2$, and $M(NO)_2M$ (M = Li, Na, and Mg)[a]

species	elec. state	point group	geometry (Å, deg)		isotopic freq, cm^{-1} (intensities, km/mol)[b]		
					$^{14}N^{16}O$	$^{15}N^{16}O$	$^{15}N^{18}O$
Li(NO)	$^3A''$	C_s	Li−N: 1.888, Li−O: 1.813,	a′	1391.4(97)	1367.0	1329.0
			N−O: 1.271, ∠NLiO: 40.1	a′	679.8(139)	677.8	673.9
				a′	352.9(25)	348.8	342.5
Li(NO)Li	$^2B_1$	C_{2v}	N−O: 1.439,	a_1	913.1(53)	899.1	877.3
			Li−O: 1.746,	b_2	827.3(276)	822.0	816.2
			Li−N: 1.811	a_1	674.1(31)	673.1	669.8
				b_2	641.7(9)	634.6	620.9
				a_1	409.0(154)	406.5	403.4
				b_1	173.5(171)	172.8	170.8
$Li(NO)_2$ [c]	$^2B_1$	C_{2v}	N−N: 1.386,	a_1	1326.1(67)	1303.6	1266.0
			N−O: 1.266,	b_2	1270.8(253)	1243.0	1217.9
			Li−O: 1.834,	b_2	935.1(63)	916.7	894.2
			∠O−Li−O: 83.9°,	a_1	833.3(0)	805.4	805.0
			∠Li−O−N: 113.1°,	a_1	620.6(127)	620.4	610.2
			∠O−N−N: 114.9°	b_2	512.3(19)	511.6	504.2
				a_1	461.3(18)	460.2	440.6
				a_2	251.5(0)	244.9	241.8
				b_1	230.5(56)	229.3	223.6
$Li(NO)_2Li$ [d]	^1A_g	C_{2h}	N−N′: 1.273, N−O: 1.342,	a_g	1369.2(0)	1323.2	1322.7
			Li−O: 1.816, Li−N: 2.261,	a_g	1238.1(0)	1205.0	1190.8
			Li−N′: 1.974, ∠ONN′: 113.9,	b_u	1078.1(509)	1058.9	1031.4
			∠NLiO: 36.4, ∠N′NLi: 60.5[e]	a_g	733.7(0)	731.9	698.7
				b_u	607.9(254)	607.5	595.0
				a_g	583.2(0)	581.9	573.7
				b_u	520.6(66)	511.8	504.5
Na(NO)	$^3A''$	C_s	Na−N: 2.233, Na−O: 2.201,	a′	1378.6(232)	1354.3	1316.7
			N−O: 1.269, ∠NNaO: 33.3	a′	385.2(44)	380.6	378.3
				a′	249.4(2)	246.6	238.9
$Na(NO)_2Na$ [d]	^1A_g	C_{2h}	N−N′: 1.277, N−O: 1.332,	a_g	1313.7(0)	1269.6	1269.1
			Na−O: 2.179, Na−N: 2.629,	a_g	1206.2(0)	1174.3	1159.6
			Na−N′: 2.283, ∠ONN′: 116.1,	b_u	1083.6(584)	1064.0	1035.5
			∠NNaO: 30.4, ∠N′NNa: 60.3[e]	a_g	713.4(0)	710.4	674.6
				b_u	534.6(14)	526.8	510.0
				a_g	346.1(0)	345.3	337.0
				b_u	361.1(96)	358.1	354.1
Mg(NO)	$^2A''$	C_s	Mg−O: 2.173, N−O: 1.196,	a′	1567.0(1708)	1540.3	1496.2
			∠MgNO: 128.8	a′	250.2(16)	244.1	242.0
				a′	217.0(16)	215.8	211.4
$Mg(NO)_2Mg$ [d]	^1A_g	C_{2h}	N−N′: 1.268, N−O: 1.316,	a_g	1384.9(0)	1339.0	1337.5
			Mg−N: 2.577, Mg−N′: 2.303,	a_g	1209.3(0)	1177.2	1162.8
			Mg−O: 2.052, ∠ONN′: 115.3,	b_u	1128.7(194)	1108.6	1078.5
			∠NMgO: 30.4, ∠N′NMg: 63.2[e]	a_g	753.2(0)	749.6	712.4
				b_u	566.1(9)	556.0	541.1
				a_g	401.9(0)	401.4	392.0
				b_u	349.8(77)	347.6	342.3

[a] DFT calculation, B3LYP functional and 6-311+G* basis set. [b] Intensities only listed for the $^{14}N^{16}O$ sample. Highest seven frequencies listed for $Li(NO)_2Li$, and their corresponding bands for $M(NO)_2M$ (M = Na and Mg). [c] The $^2A_1$ state, C_{2v} cis structure is 16.7 kcal/mol higher; the $^2A'$ state, C_s trans structure is 18.2 kcal/mol higher. [d] Dissociation energies for the reactions: $M(NO)_2M \rightarrow 2M(NO)$ are 68.8, 68.0, and 52.4 kcal/mol for M = Li, Na, and Mg, respectively. [e] N′ refers to the nitrogen atom in the other M(NO) unit.

1358.3 cm^{-1} bands. Both Li−*cis*-$(NO)_2$ and Li−*trans*-$(NO)_2$ were calculated and the cis isomer is lower in energy by 18.2 kcal/mol presumably because of more intimate Li interaction with more of the $(NO)_2$ subunit in this configuration. The Li−*cis*-$(NO)_2$ species gave a strong b_2 frequency at 1270.8 cm^{-1}. A C_{2v} structure for Li(NO)Li and C_{2h} structure for $Li(NO)_2Li$ were also converged, and the parameters are also given in Table 2. The BPW91 functional gave 1−11 cm^{-1} lower b_u frequencies and 0.02−0.04 Å longer bonds for the $M(NO)_2M$ species. The $Li(NO)_2Li$ molecule is 68.8 kcal/mol lower than two $^3A''$ Li(NO) subunits. Figure 4 illustrates the structures of the lithium species calculated here, and Table 4 contrasts the Mulliken[30] and natural bond orbital[40] atomic charges and shows that these molecules exhibit a high degree of ionic character based on the more reliable NBO analysis.[41]

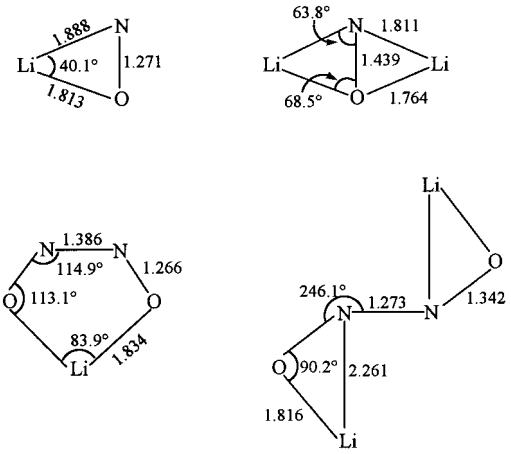

Figure 4. Structures of $Li_x(NO)_y$ species calculated at the B3LYP/6-311+G level (bond lengths in Å).

(40) Reed, A. J.; Curtiss, L. A.; Weinhold, F. *Chem. Rev.* **1988**, *88*, 899.
(41) Frenking, G.; Frohlich, N. *Chem. Rev.* **2000**, *100*, 717.

Table 4. Atomic Charges (e) in the $M_x(NO)_y$ Species (M = Li, Na) Calculated at the B3LYP/6-311+G* Level

	Mulliken[a]			natural bond orbital[b]		
molecule	M	N	O	M	N	O
Li(NO), $^3A''$	+0.44	−0.24	−0.20	+0.91	−0.31	−0.60
Li(NO)Li, $^2B_1$	+0.31	−0.27	−0.35	+0.91	−0.88	−0.94
$Li(NO)_2$, $^2B_1$	+0.50	−0.12	−0.13	+0.94	+0.09	−0.56
$Li(NO)_2Li$, ^1A_g	+0.33	−0.12	−0.21	+0.89	−0.77	−0.12
Na(NO), $^3A''$	+0.67	−0.41	−0.26	+0.92	−0.33	−0.59
$Na(NO)_2Na$, ^1A_g	+0.67	−0.24	−0.43	+0.85	−0.10	−0.75

[a] Reference 30. [b] Reference 40.

Recent quantum chemical calculations of *cis*- and *trans*-$N_2O_2^{2-}$ dianions have suggested that the trans form is slightly more stable;[42] however, such calculations with limited atomic orbital basis sets may not provide a reasonable description of the isolated $N_2O_2^{2-}$ dianion.[2,5] We attempted to calculate the Li(Ar)$(NO)_2$(Ar)Li molecule, but the calculation failed to converge. We performed several approximate calculations with fixed dimensions and the most promising involved a fixed Li−O distance at 5.58 Å (sum of the Li−O distance and one argon diameter), fixed N−O−Li angle at 90°, and constrained Ar to lie on the line between O and Li. We found three low (<42 cm^{-1}) imaginary frequencies and a strong b_u mode at 1316 cm^{-1} (1318 cm^{-1} for the Na counterpart), which is more appropriate for an $N_2O_2^-$ species. This structure is 161 kcal/mol *higher* than 2 Ar atoms and $Li(NO)_2Li$ and shows *less* charge transfer. Next we calculated Li−$(NO)_2$−Li with fixed Li−O distances (4.0 Å) and Li−O−N angles (100 and 120°), and obtained two low imaginary frequencies and b_u modes of 1332 ± 1 cm^{-1}; these structures with more remote Li atoms are 160 ± 1 kcal/mol higher than the optimized $Li(NO)_2Li$ species. Finally, we reduced the Li basis to 6G (1s function) with 6-31G* on N, O and fixed the Li−O distance (5.0 Å) and N−O−Li angle (90°); this calculation gave five low-frequency imaginary Li motions, a 1010 cm^{-1} b_u frequency, and Mulliken charges of +1 on Li (of course), −0.18 on N, and −0.82 on O.

Assignment of the 1404.1, 1392.6, 1390.6, and 795.3 cm^{-1} Absorptions. The sharp 1404.1 cm^{-1} absorption appears on annealing to 35 and 40 K at the expense of Li(NO) under conditions where NO decreases and $(NO)_2$ increases. The 1404.1 cm^{-1} band forms a 1/2/1 triplet at 1404.1, 1391.3, and 1381.4 cm^{-1} in $^{14}NO + {}^{15}NO$ samples and at 1381.4, 1360.4, and 1344.1 cm^{-1} in $^{15}N^{16}O + {}^{15}N^{18}O$ experiments. These observations confirm the participation of two equivalent NO subunits in this vibrational mode. The $^{14}NO/^{15}NO$ and $^{15}N^{16}O/^{15}N^{18}O$ ratios 1.0164 and 1.0278 are appropriate for an N−O vibration. The C_{2v} $Li(NO)_2$ molecule is calculated to absorb strongly at 1270.8 cm^{-1} just above the isolated $(NO)_2^-$ species,[36] so more metal atoms are involved. Accordingly, the 1404.1 cm^{-1} band and 1392.6 cm^{-1} site are probably due to $Li(Ar)_x(NO)_2(Ar)_xLi$, and the analogous Na species absorbs at 1390.6 cm^{-1}. The spectra in Figure 1e,f,g and Figure 2d,e,f show that annealing to 35 K produces this species, UV photolysis decreases these absorptions in favor of the 1028.5 cm^{-1} band, and annealing to 40 K produces more of this $M(Ar)_x(NO)_2(Ar)_xM$ species.

The 885.6, 795.3, and 415.5 cm^{-1} bands assigned[17] to $(Li^+)(NO^{2-})(Li^+)$ are well modeled by similar calculations, which predicted infrared absorptions at 878.1, 800.6, and 399.0 cm^{-1} at the BPW91 level[20] and at 931.1, 827.3, and 409.0 cm^{-1} at the B3LYP level for the a_1 $(N-O)^{2-}$ and b_2 and a_1 Li−(NO) stretching modes.

The weak 1055 cm^{-1} band that appears on annealing (Figure 1g) is the only possible assignment for the $Li(NO)_2Li$ molecule, but this can only be tentative without isotopic data. The analogous $Ag(NO)_2Ag$ molecule has been observed as a major product at 1117 cm^{-1} in solid argon and predicted at 1146 cm^{-1} by DFT calculations.[43]

Identification of the 1028.5 cm^{-1} Absorber. The 1028.5 cm^{-1} absorption becomes a sharp triplet at 1028.5, 1019.2, and 1010.4 cm^{-1} with $^{14}N^{16}O + {}^{15}N^{16}O$ and a sharp triplet at 1010.4, 996.5, and 983.7 cm^{-1} with $^{15}N^{16}O + {}^{15}N^{18}O$ (Figure 3). The $^{14}N^{16}O/^{15}N^{16}O$ ratio (1.0179) and $^{15}N^{16}O/^{15}N^{18}O$ ratio (1.0271) are nearly the same as the ratios for diatomic NO (1.0179 and 1.0277). This clearly demonstrates the involvement of two equivalent NO oscillators in the 1028.5 cm^{-1} vibrational mode.

The *cis*-$(NO)_2$ dimer absorbs at 1776.2 cm^{-1} and the *cis*- and *trans*-$(NO)_2^-$ anions at 1222.7 and 1221.0 cm^{-1} (antisymmetric N−O modes). The 1028.5 cm^{-1} band requires still weaker N−O bonds and is in almost exact agreement with the b_u fundamental (1030 cm^{-1}) for *trans*-$(NO)_2^{2-}$ in solid $Na_2N_2O_2$.[21−23] Our DFT frequency calculations predict 1078.1 and 1083.6 cm^{-1} for the strongest modes of the $Li(NO)_2Li$ and $Na(NO)_2Na$ molecules and the $^{14}N^{16}O/^{15}N^{16}O$ and $^{15}N^{16}O/^{15}N^{18}O$ isotopic frequency ratios (1.0181, 1.0184 and 1.0267, 1.0275) almost exactly match the observed ratios. However, the 1028.5 cm^{-1} absorption is clearly independent (±0.1 cm^{-1}) of the metal employed. Hence, the metal cations are not mechanically coupled with the $N_2O_2^{2-}$ vibration, and the $N_2O_2^{2-}$ dianion observed here must be insulated by the argon matrix. How, then, does the isolated $N_2O_2^{2-}$ dianion not undergo autoionization to $N_2O_2^-$ and e^- or spontaneous decomposition to a pair of NO^- anions? There must be electrostatic stabilization by M^+ cations separated by one or two layers of argon atoms from the $N_2O_2^{2-}$ dianion observed here.

Our attempts to model the observed $(Li^+)(Ar)_x(N_2O_2^{2-})(Ar)_x(Li^+)$ species have been only partially successful. Although the $Li(NO)_2Li$ and $Na(NO)_2Na$ calculations predict strong b_u infrared absorptions at 1078.1 and 1083.6 cm^{-1}, respectively, which scale appropriately[44] (by 0.95) to the observed 1028.5 cm^{-1} frequency, there is too much calculated metal dependence. Accordingly, the metal was moved further away with a concomitant increase in energy and b_u frequency. The same was found when Ar atoms were placed between Li, $(NO)_2$, and Li. However, when the lithium basis is restricted to 1s functions, appropriate charge transfer over a fixed remote distance does occur and an appropriate b_u dianion frequency is found. We were not able to calculate the ionic species reached by UV photolysis, namely $(Li^+)(Ar)_x(N_2O_2^{2-})(Ar)_x(Li^+)$, which is physically stable and separated by a barrier from the more stable $Li(NO)_2Li$ molecule, but we have offered several approximate models to support the argon matrix spectrum of $N_2O_2^{2-}$. Our system is similar to the stabilization of the sulfate dianion by an alkali cation as $M^+(SO_4^{2-})$[45] although we have two metal cations and two or more argon insulators around $N_2O_2^{2-}$.

Reactions in the Matrix. During condensation, diffusion of reagents allows spontaneous reactions and the following products discussed above are formed: $(NO)_2$, Li(NO), and Li(NO)Li.

$$NO + NO \rightarrow cis\text{-}(NO)_2 \quad (1)$$

$$Li + NO \rightarrow Li(NO) \quad (2)$$

(42) Snis, A.; Panas, I. *Chem. Phys.* **1997**, *221*, 1.

(43) Citra, A.; Andrews, L. *J. Phys. Chem. A*, **2001**, in press (Ag + NO).

(44) Bytheway, I.; Wong, M. W. *Chem. Phys. Lett.* **1998**, *282*, 219.

(45) Wang, X. B.; Ding, C. F.; Nicholas, J. B.; Dixon, D. A.; Wang, L. S. *J. Phys. Chem. A* **1999**, *103*, 3423.

$$Li(NO) + Li \rightarrow Li(NO)Li \quad (3)$$

$$Li(NO) + NO + Li + XAr \rightarrow Li(Ar)_x(NO)_2(Ar)_xLi \quad (4)$$

However, under these very cold conditions for condensing argon, some Li atoms are trapped in the 7 K argon matrix separated by one or two layers of argon atoms from $(NO)_2$ as suggested by reaction 4 and Scheme 1. The known size of the $(NO)_2$ dimer allows a comfortable fit into a two-argon vacancy.[46,47] If photoelectron transfer occurs with one argon atom insulating, 7.5 Å separation (two argon diameters, i.e., 3.76 + 3.76 Å) between Li^+ and $N_2O_2^{2-}$ centers provides electrostatic stabilization of approximately 44 kcal/mol per Li^+ or 88 kcal/mol total, which is an overestimate of the separation and an underestimate of the stabilization. Simply squeezing one argon atom between each Li and $(NO)_2$ in $Li(NO)_2Li$ predicts a 5.6 Å separation and a stabilization of approximately 59 kcal/mol per Li^+ or 118 kcal/mol total. Hence, the $N_2O_2^{2-}$ dianion formed here by photoionization of metal atoms is isolated and insulated by the argon matrix (one or two layers) from the metal cations that stabilize the dianion. Irradiation with 240 nm photons is capable of direct ionization of Li with a 1700 cm^{-1} red shift by the matrix[48] and direct ionization of Na with no matrix shift. In contrast photolysis with red and near-infrared radiation destroys the $N_2O_2^{2-}$ species most likely by a reverse electron-transfer process. The slight *decrease* in $(NO)_2$ on formation of $N_2O_2^{2-}$ and an *increase* on photodestruction are consistent with the reversible photochemical reaction 5. The slight increase in the isolated $N_2O_2^-$ absorption with UV photolysis that forms $N_2O_2^{2-}$ and visible photolysis that destroys $N_2O_2^{2-}$ (Table 2) suggests that reaction 5 may proceed through isolated $N_2O_2^-$ anion[36] in two electron-transfer steps. The isolated $N_2O_2^{2-}$ dianion is extremely sensitive to photodetachment by red light.

$$Li(Ar)_x(NO)_2(Ar)_xLi \underset{\lambda > 630\ nm}{\overset{240-380\ nm}{\rightleftharpoons}} (Li^+)(Ar)_x(N_2O_2^{2-})(Ar)_x(Li^+) \quad (5)$$

Conclusions

Ultraviolet irradiation of a rigid 7 K argon matrix containing alkali or alkaline earth metal atoms and $(NO)_2$ isolated from each other by one or two layers of argon forms $N_2O_2^{2-}$ insulated from two M^+ by argon, and red visible photolysis reverses the electron-transfer process probably involving the $N_2O_2^-$ anion intermediate. The isolated $N_2O_2^{2-}$ dianion is identified from isotopic substitution and isotopic mixtures, which show that the new 1028.5 cm^{-1} metal independent absorption involves two equivalent NO subunits. Our DFT calculations model only the $M(NO)_2M$ species which predict strong 1078.1 and 1083.6 cm^{-1} bands for Li and Na, respectively. The spectrum of solid $Na_2N_2O_2$ exhibits a 1030 cm^{-1} infrared band,[13-15] which strongly supports the present assignment.

This work presents the first infrared spectroscopic measurement on a dianion sufficiently isolated from cations that no cation perturbation is observed in the dianion spectrum. The electrostatic stabilization of $N_2O_2^{2-}$, which is probably unstable in the gas phase, is made possible by metal cations separated by one or two insulating layers of argon in the rigid 7 K matrix.

Scheme 1

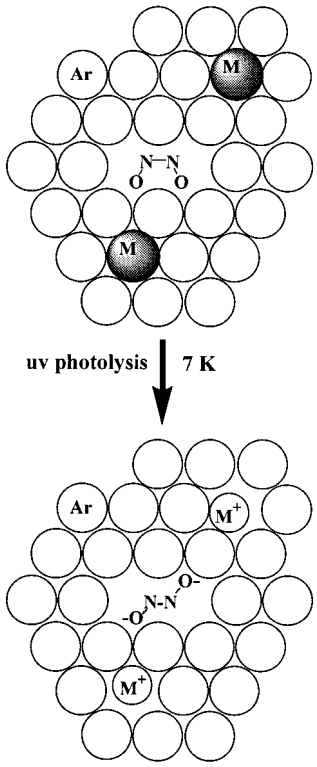

Acknowledgment. We gratefully acknowledge the National Science Foundation and the Petroleum Research Fund for support of this research, C. O. Trindle for suggesting and performing the lithium 6G basis set calculation, and C. W. Bauschlicher, Jr., for helpful correspondence.

JA0029331

(46) East, A. L. L. *J. Chem. Phys.* **1998**, *109*, 2185 and references therein.
(47) Pollack, G. L. *Rev. Mod. Phys.* **1964**, *36*, 748.
(48) Gedanken, A.; Raz, B.; Jortner, J. *J. Chem. Phys.* **1973**, *58*, 1178.